

**Past and Future Climate Variability Uncertainties in the Global Carbon Budget using the MPI Grand Ensemble**

T. F. Loughran<sup>1</sup>, L. Boysen<sup>3</sup>, A. Bastos<sup>1,2</sup>, K. Hartung<sup>1,\*</sup>, F. Havermann<sup>1</sup>, H. Li<sup>3</sup>, J. E. M. S. Nabel<sup>3</sup>, W. A. Obermeier<sup>1</sup>, and J. Pongratz<sup>1</sup>

<sup>1</sup>Dept. of Geography, Ludwig Maximilian University, Munich, Germany.

<sup>2</sup>Max Planck Institute for Biogeochemistry, Jena, Germany.

<sup>3</sup>Max Planck Institute for Meteorology, Hamburg, Germany.

\*Now at: Deutsches Zentrum für Luft- und Raumfahrt, Institut für Physik der Atmosphäre, Oberpfaffenhofen, Germany.

**Contents of this file**

Figures S1  
Text S1 describing Figure S2  
Figures S2  
Figures S3  
Figures S4  
Figures S5  
Figures S6  
Figures S7

**Introduction**

The following document contains supporting text and figures for the analysis in the main article. The MPI-GE carbon budget is presented in various forms: there is an unstacked presentation of the budget terms (Figure S1), spatial maps of ensemble standard deviation (Figure S2), a budget composed using CMIP5 emissions (Figure S3), comparisons to the future emissions and the 2020 Global Carbon Budget (Figure S4), demonstration of the exceedance probability calculation (Figure S5 and S6) and the ensemble sub-sampling for terms not presented in the main text (Figure S7).

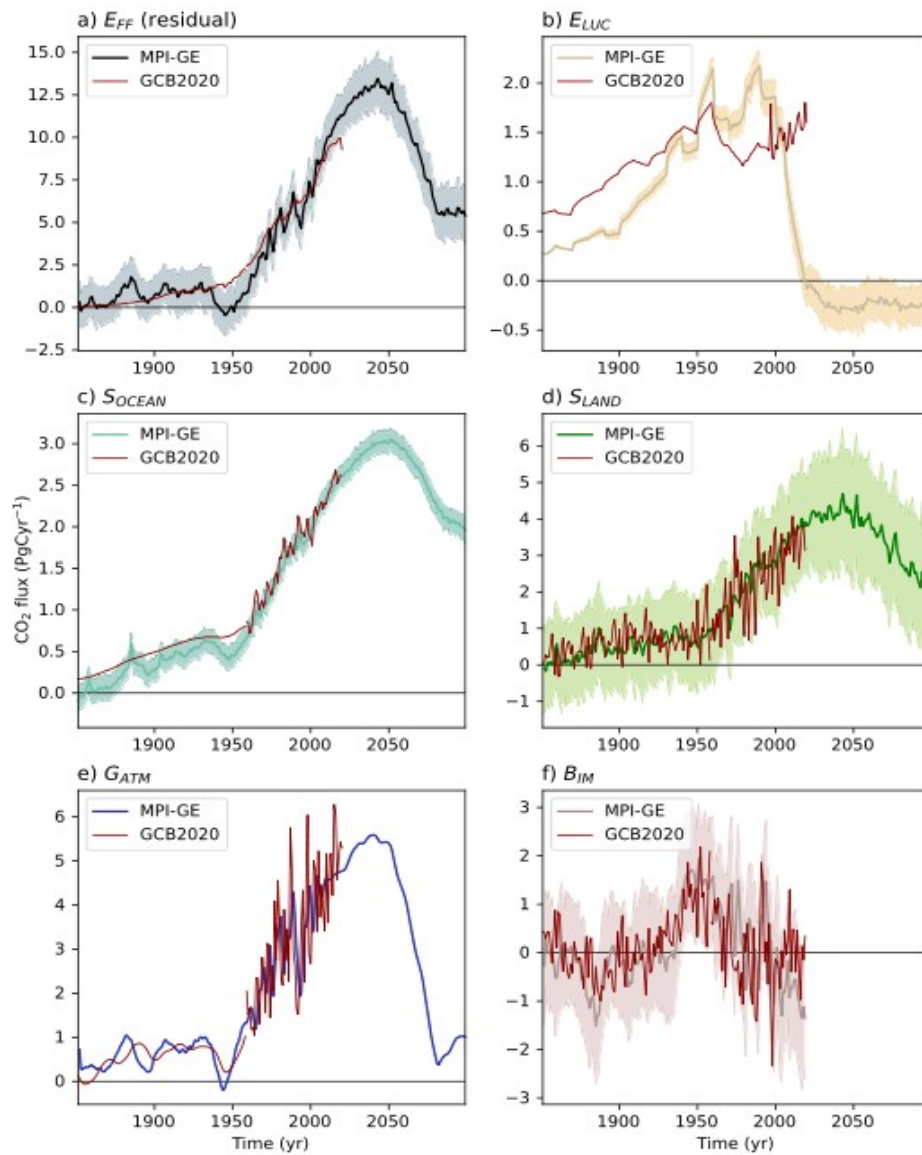


**Figure S1.** Unstacked MPI-GE carbon budget terms. The shaded region shows the  $\pm 1\sigma$  uncertainty range around the MPI-GE ensemble mean. The fine gray lines mark the corresponding GCB2020 budget terms. Panel f) shows the simulated  $B_{IM}$  term using the budget in Figure S3.

**Text S1.**

The spatial distribution of the standard deviation may reveal the regions of  $S_{\text{LAND}}$  and  $E_{\text{LUC}}$  that are most sensitive to changes in the climate under the RCP4.5 scenario. Figure S2 shows the standard deviation of  $S_{\text{LAND}}$  and  $E_{\text{LUC}}$  averaged over the last decade of the RCP4.5 scenario. The regions of  $S_{\text{LAND}}$  with the largest variations are tropical regions that can store large masses of carbon in particular in plant biomass (such as the Amazon region in South America, the Congo region in equatorial Africa, and Southeast Asia), and are also strongly influenced by ENSO. Vegetation in all of these regions is known to be sensitive to variations in climate modes (Dannenberg et al. 2015; Poulter et al. 2014; Zhang et al. 2019; Bastos et al. 2018). There are also moderate variances found in extra-tropical regions that are affected by internal climate variability, such as North America, Europe and Australia. Regions that are not sensitive to climate variations are the highly arid regions of Saharan Africa, Central Asia, and the boreal tundra regions. The distribution patterns of sensitivity are similar for  $E_{\text{LUC}}$  (since the cleared biomass is affected by internal climate variations in the same way as the biomass contributed by  $S_{\text{LAND}}$  is, although the magnitude of the variations are much smaller, and the largest values are focused on regions with high land-use change (which are scenario dependent). The  $E_{\text{FF}}$  and  $E_{\text{LUC}}$  are not directly affected by internal climate variations, but the historical exceedance probabilities are nonetheless presented in Figure S7.

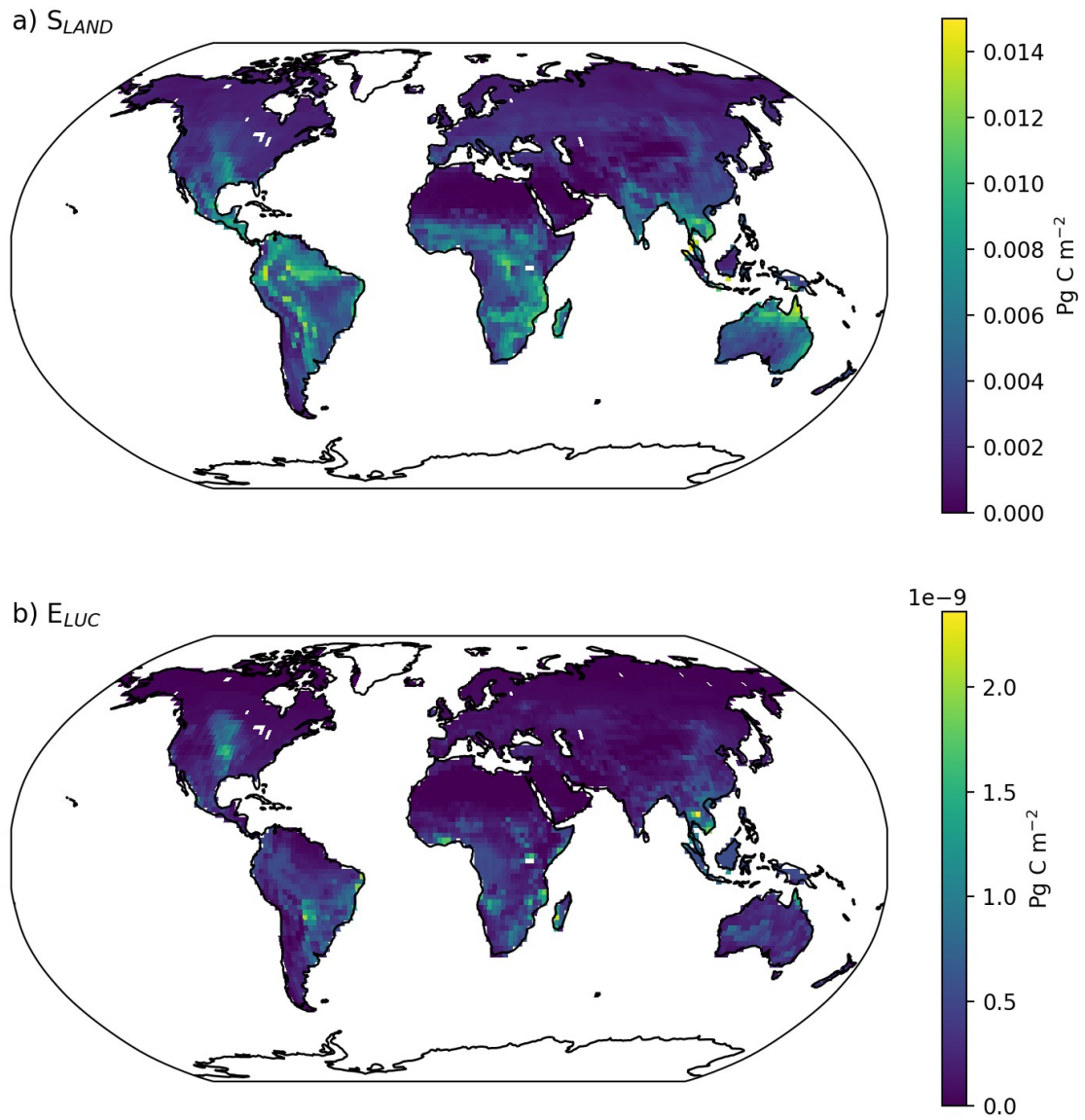


**Figure S2.** Maps of MPI-GE  $S_{LAND}$  and  $E_{LUC}$  standard deviation averaged for the final decade of the RCP4.5 scenario.

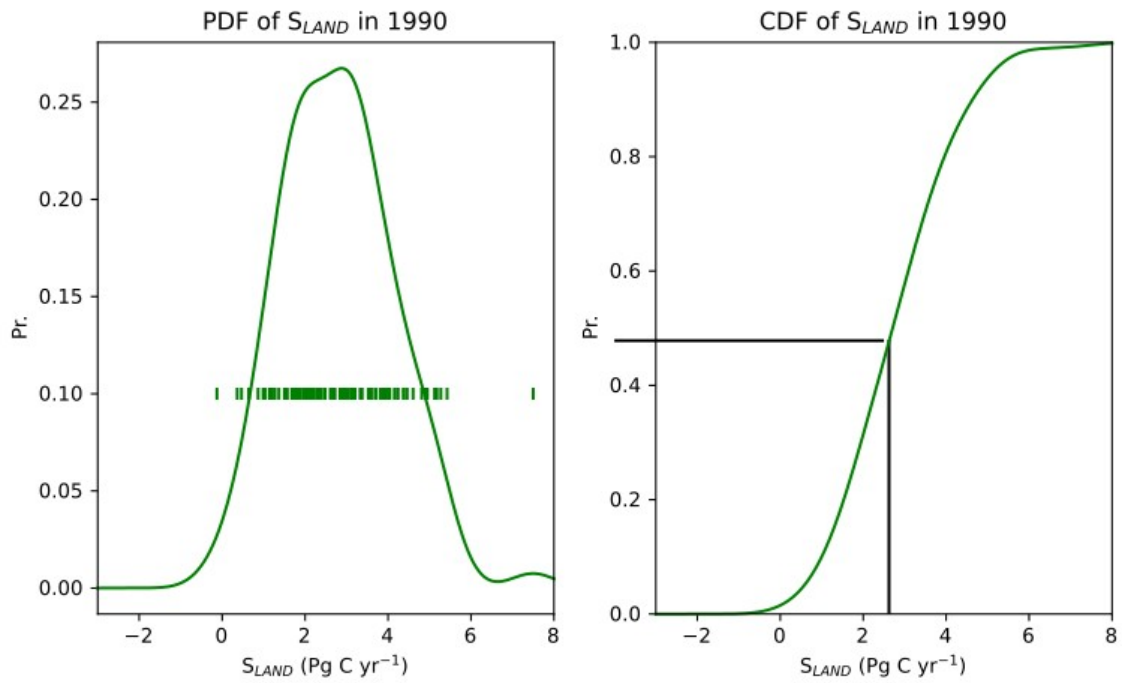


**Figure S3.** Probability of occurrence calculation of  $S_{LAND}$  for a single year 1990. The probability distribution function of the MPI-GE is on the left and the cumulative distribution function is on the right. Dots mark the  $S_{LAND}$  values for individual ensemble members. The 1990 GCB2020 value is the vertical line and its corresponding cumulative probability of occurrence is the horizontal line.

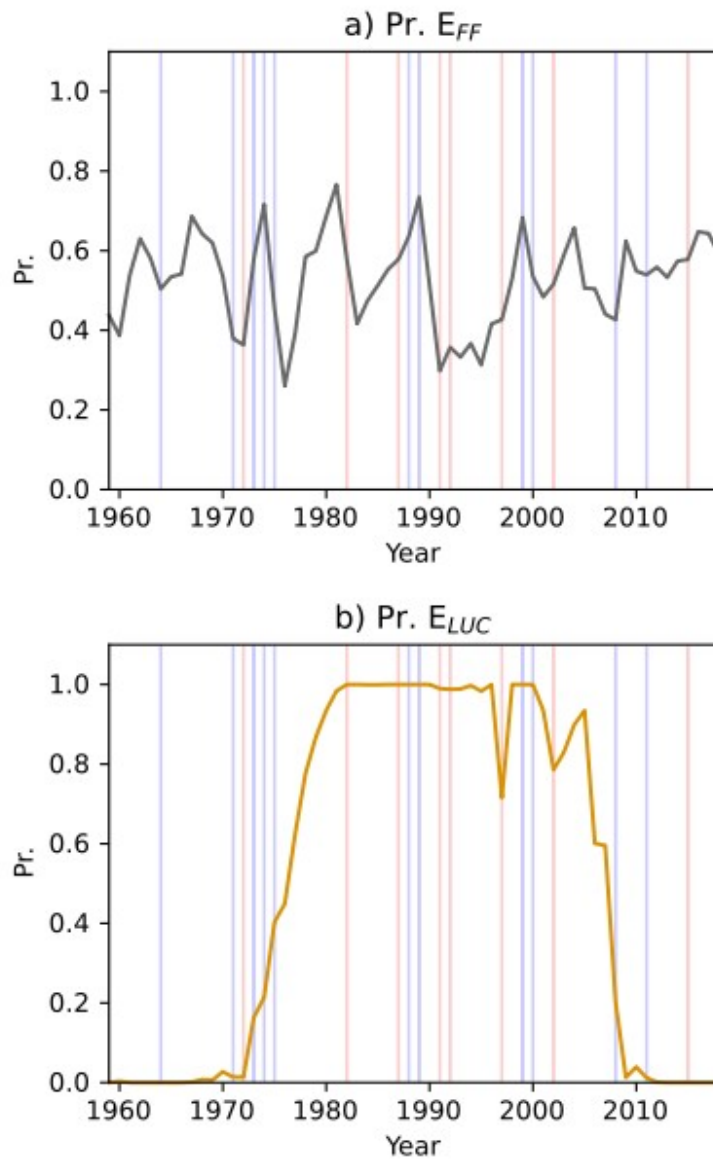


**Figure S4.** Probability of exceedance that the MPI-GE anthropogenic carbon fluxes are greater than the historical GCB2020 mean. The vertical lines mark El Niño (red) and La Niña (blue) years where Niño 3.4 index is greater than 1 standard deviation from the mean.

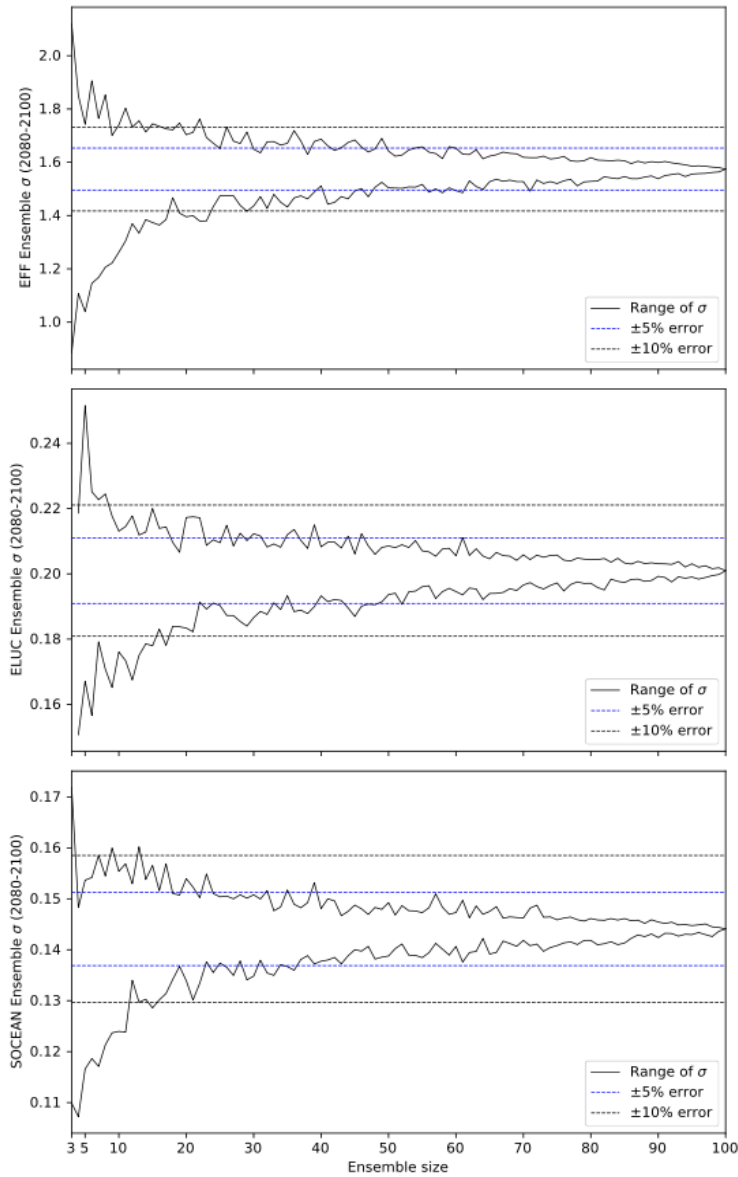


**Figure S5.** Range of standard deviation of the ensemble sub-samples for  $E_{FF}$  (top),  $E_{LUC}$  (middle) and  $S_{OCEAN}$  (bottom). Blue dashed lines mark the accuracy range of the subsample estimates for  $\pm 5\%$  error and the black dotted lines mark the accuracy range of the subsamples estimates for  $\pm 10\%$  error.

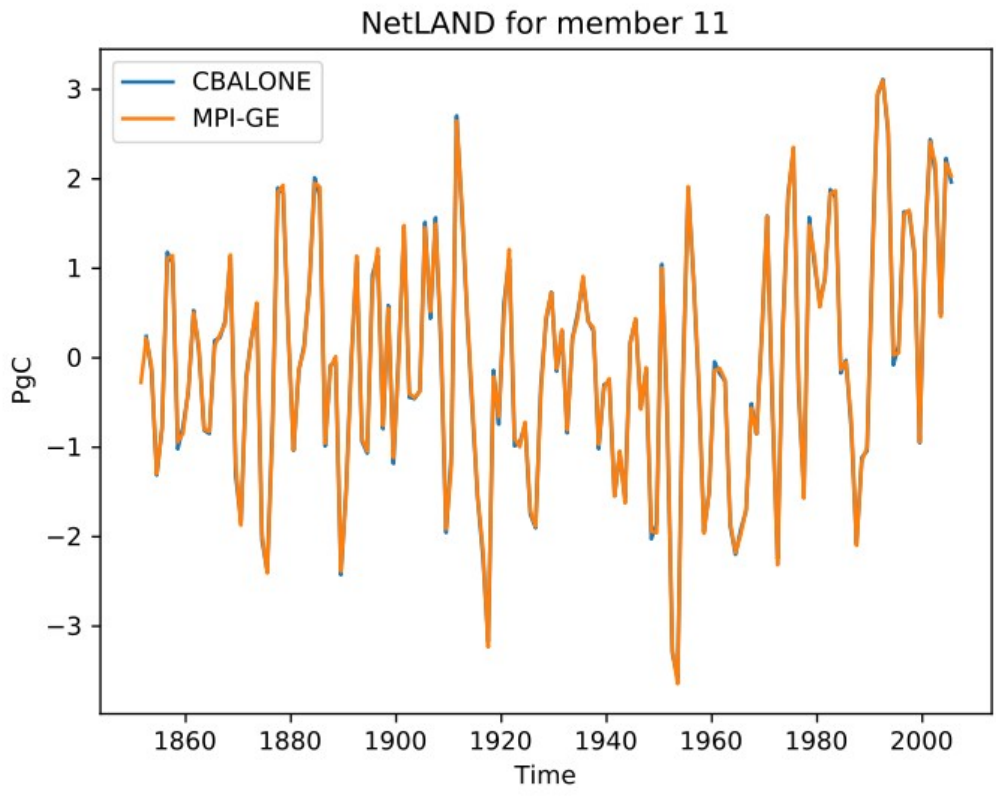


**Figure S6.** Net land-atmosphere exchange expressed as NBP for the historical period. MPI-GE and CBALONE with land use change are shown for comparison.